


Persistent Sampling of Vertically Migrating Biological Layers by an Autonomous Underwater Vehicle Within the Beam of a Seabed-Mounted Echosounder

Yanwu Zhang , Senior Member, IEEE, Brian Kieft, Brett W. Hobson, Ben-Yair Raanan, Samuel S. Urmy, Kathleen J. Pitz, Christina M. Preston, Brent Roman, Kelly J. Benoit-Bird, James M. Birch, Francisco P. Chavez, and Christopher A. Scholin

Abstract—Many pelagic animals, such as krill, lanternfish, and cephalopods, migrate to deep water at dawn to avoid visual predators during daylight hours and move up toward the sea surface at dusk to search for food. This behavior is termed “diel vertical migration.” Migrating animals graze on phytoplankton or zooplankton and in turn serve as food for higher trophic levels, hence providing a key mechanism for carbon export via this migration. These animals are often observed as sound-scattering layers by echosounders, but the animals causing the acoustic scattering are difficult to identify using acoustics alone. In a spring 2019 experiment in Monterey Bay, we deployed autonomous underwater and surface vehicles over a seabed-mounted upward-looking echosounder to collect environmental DNA (eDNA) with the goal of identifying the vertically migrating animals. The echosounder was installed at 890-m depth on the Monterey Accelerated Research System (MARS) seabed cabled ocean observatory, providing real-time data of acoustic backscatter from the full water column. One long-range autonomous underwater vehicle (LRAUV) carrying a Third-Generation Environmental Sample Processor (3G-ESP) acquired water samples from a sequence of layers from near surface down to ~290 m as directed by the distribution of animals observed by the echosounder. During the sampling of each layer, the LRAUV ran on a tight circular yo-yo trajectory directly above the echosounder, remaining in its beam by acoustically tracking a station-keeping Wave Glider on the sea surface marking the echosounder’s latitude and longitude. The persistent and simultaneous acoustic observation and eDNA acquisition enables identification of animals at precise locations to better understand their vertical migration behaviors. We present the methods and the system performance in the experiment.

Index Terms—Autonomous underwater vehicle (AUV), biological layers, echosounder, Environmental Sample Processor (ESP), sampling, Wave Glider.

Manuscript received October 24, 2019; revised February 19, 2020; accepted March 18, 2020. Date of publication May 14, 2020; date of current version April 14, 2021. This work was supported by the David and Lucile Packard Foundation. (Corresponding author: Yanwu Zhang.)

Associate Editor: R. Bachmayer.

Yanwu Zhang, Brian Kieft, Brett W. Hobson, Ben-Yair Raanan, Kathleen J. Pitz, Christina M. Preston, Brent Roman, Kelly J. Benoit-Bird, James M. Birch, Francisco P. Chavez, and Christopher A. Scholin are with the Monterey Bay Aquarium Research Institute, Moss Landing, CA 95039, USA (e-mail: yzhang@mbari.org).

Samuel S. Urmy is with the Alaska Fisheries Science Center, National Marine Fisheries Service, National Oceanic and Atmospheric Administration, Seattle, WA 98115, USA.

Digital Object Identifier 10.1109/JOE.2020.2982811

I. INTRODUCTION

MANY pelagic zooplankton and micronekton follow a daily cycle of vertical migration, feeding at the surface under cover of darkness and retreating to deeper water during the day to avoid visual predators [1], [2]. This diel vertical migration connects the photic zone to mesopelagic ecosystems, and plays an important role in transporting nutrients and carbon across the thermocline. These daily migrations were first identified using sonar, resulting in the term “sound-scattering layers (SSLs)” [3], [4], and they are of major ecological and biogeochemical importance [5], [6]. The species that make up these SSLs usually cannot be determined using acoustics alone. Therefore, additional ship-based direct sampling (e.g. nets and optics) is typically required to identify organisms and ground-truth acoustic abundance estimates [7], [8]. However, when an acoustic instrument is deployed for long periods on moorings or observatory nodes, obtaining sufficient direct samples becomes a challenge.

As marine animals move through the water they shed particles, skin, or excrement that contain DNA. These traces can be extracted and are collectively known as environmental DNA (eDNA). The eDNA from water samples can therefore be used to detect animals as well as single-celled organisms, ranging from microbes to zooplankton, fish, and whales [9]. In this paper, we demonstrate the use of an autonomous underwater vehicle (AUV) to acquire eDNA samples within the acoustic beam of a seabed-mounted upward-looking echosounder. These techniques allow the biological constituents of the SSLs to be identified autonomously over multiple cycles of vertical migration with fine vertical resolution.

An upward-looking acoustic package [10] based on a split beam 38-kHz Simrad EK60 echosounder was installed at the Monterey Accelerated Research System (MARS) ocean observatory to continuously observe the distribution and abundance of animals in the water column. The MARS cabled observatory is located outside the mouth of Monterey Bay on the seafloor at 890-m depth.¹ Its central hub has eight ports for instruments. The

¹<https://www.mbari.org/at-sea/cabled-observatory/>

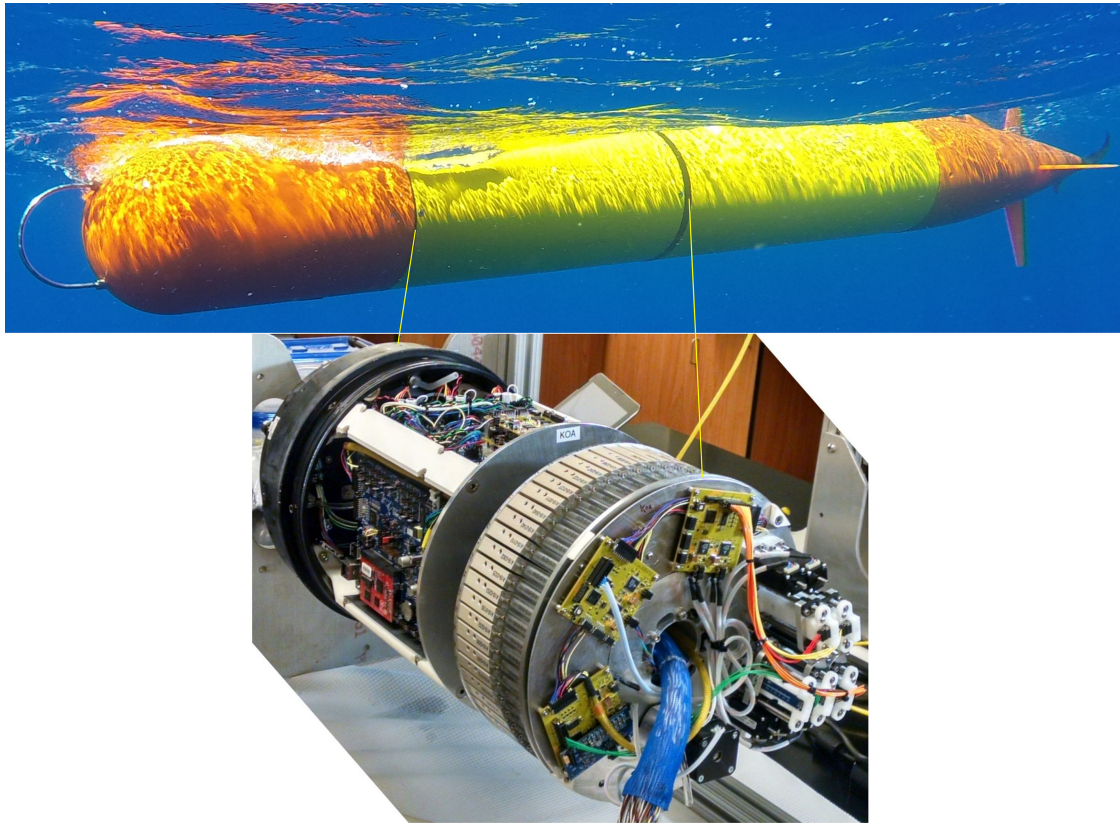


Fig. 1. LRAUV with a 3G-ESP installed in the vehicle's fore-mid section (photo courtesy of Elisha Wood-Charlson).

observatory is connected to shore through a 52-km optoelectrical cable that delivers electrical power to attached instruments and transmits data from those instruments to shore in real time.

Data from the echosounder sent to the onshore scientists are combined to form an “echogram” (i.e., a composite visual representation of the echoes over time) revealing processes like the vertical migration of layers of animals in the water. The echosounder emits focused sound pulses upward every 2.5 s and receives echoes backscattered from pelagic animals. The distance from the echosounder to the scattering object is derived from the two-way travel time of the echo and, when the objects are isolated, the phase differences of the echo signal between the different receiving channels can be used to localize the objects within the echosounder's beam [11]. Most 38-kHz scattering at this site is due to layers of micronekton and small fishes, including krill, myctophids, sergestid shrimp, siphonophores, and juvenile Pacific hake [4]. For dispersed animals, the echo amplitude is (to the first order) proportional to the number of animals in the water [12], giving a proxy for animal density through the water column. Over time, the marine animals' diel vertical migration is represented on the echogram.

To determine the biological composition of the acoustic scattering layers, we deployed a Tethys-class long-range AUV (LRAUV) equipped with a Third-Generation Environmental Sample Processor (3G-ESP) [13], [14] (see Fig. 1) to acquire water samples directly above the echosounder for the eDNA analysis [15]. The LRAUV is 3.2 m long and 0.3 m in diameter at the

midsection. It can run from 0.5 to 1 m/s using a propeller. Using a primary battery, the vehicle has demonstrated a range of 1800 km (three-week duration) at 1-m/s speed [16]. Long range is realized by minimizing propulsion power consumption through an innovative design of a low-drag body and a high-efficiency propulsion system [17]. In addition, by using a buoyancy engine, the vehicle is capable of ballasting to neutral buoyancy and drifting in a lower power mode. An LRAUV thus combines the mobility and speed of propeller-driven vehicles and energy savings of buoyancy-driven vehicles. An LRAUV's science sensors suite (all in the nose section) includes SBE GPCTD temperature, conductivity, and depth sensors, a WET Labs BB2FL fluorescence/backscatter sensor (chlorophyll fluorescence excitation wavelength 470 nm and emission wavelength 695 nm), an Aanderaa 4831F dissolved oxygen sensor, and an LI-COR LI-192SA photosynthetically active radiation sensor. The LRAUV software architecture uses the state-configured layered control [18], which divides the vehicle's operations into a group of behaviors assigned with hierarchical levels of priority. For each AUV mission, the vehicle runs a mission script that invokes appropriate AUV behaviors to achieve a specified goal [16], [19].

The 3G-ESP is installed in the forward pressure housing of the LRAUV. It uses cartridges to collect and process ocean samples for the molecular analysis. Up to 60 cartridges are installed on a wheel, and each cartridge contains the filters and reagents necessary for collecting and processing one sample. The cartridges connect to a central ring of valves that are part of a pumped

seawater loop. When the LRAUV mission program triggers a sampling event, the 3G-ESP rotates the motor-driven cartridge wheel to align a designated cartridge with the processing station, where power and actuators can be applied to the cartridge. The pumped seawater loop is flushed clear, and actuators open valves to direct the seawater through the cartridge, concentrating particles, small animals (<1 mm), cells, and extracellular eDNA onto the filters. A reagent is added to the sample to preserve the cellular material for later analysis in the laboratory or to extract an analyte from the sample for real-time detection and quantification. In the presented study, the filter pore size was $0.2 \mu\text{m}$, and all particulate samples were preserved onboard for subsequent analysis in a shoreside laboratory [15].

Vehicle-to-vehicle autonomous tracking is based on AUV onboard acoustic ranging and direction finding. The tracking vehicle carries an acoustic transceiver and an ultrashort baseline (USBL) array. The tracked vehicle carries an acoustic transponder. The tracking vehicle periodically emits acoustic pulses. When receiving the signal, the tracked vehicle sends a reply pulse back to the tracking vehicle. The tracking vehicle estimates the range of the tracked vehicle based on the round-trip travel time of the signal, and estimates the direction based on the phase differences at the array of hydrophones in the USBL. An early test was reported in [20]. One Odyssey IIB AUV surveyed a field in a lawnmower pattern. A second AUV navigated to follow the surveying AUV based on the estimated range and direction.

To enable LRAUV acoustic tracking, we installed a Teledyne Benthos acoustic modem in the vehicle being tracked, and a Teledyne Benthos directional acoustic transponder (DAT) in the tracking vehicle. The DAT integrates an acoustic modem and a USBL acoustic positioning system [21]. Based on the range and direction estimates of the tracked vehicle, the tracking vehicle autonomously updates its own commanded position to follow the tracked vehicle at the desired standoff distance. In a 2015 experiment in Monterey Bay, one LRAUV stayed on a targeted 10.5°C isotherm over 13 h in drift mode [22]. The isotherm depth ranged from 10 to 35 m. A second LRAUV acoustically tracked the drifting LRAUV, and ran on a circular yo-yo trajectory around it [22], [23]. The yo-yo depth range was from surface to 60 m, and the radius of the circle was 200 m. In a 2018 experiment to the north of the Hawaiian Islands, one LRAUV sampled the deep chlorophyll maximum layer at $\sim 100\text{-m}$ depth in a cyclonic eddy for four days [24]. A second LRAUV acoustically tracked the sampling LRAUV, and spiraled around it to measure the contextual water properties both horizontally and vertically (from 50 to 200 m depths). The average tracking distance was about 800 m. In both experiments, one Wave Glider also acoustically tracked the drifting or sampling LRAUV. In the tracking algorithms on the LRAUV and the Wave Glider, the tracking and tracked vehicles were considered lying on the same horizontal plane (hence the DAT-measured slant range was used as the horizontal range), given that the depth difference between the two vehicles was smaller than or comparable to their horizontal distance.

In this study, an LRAUV equipped with a 3G-ESP was required to remain in the acoustic beam of a seabed-mounted echosounder, to collaboratively observe and sample the

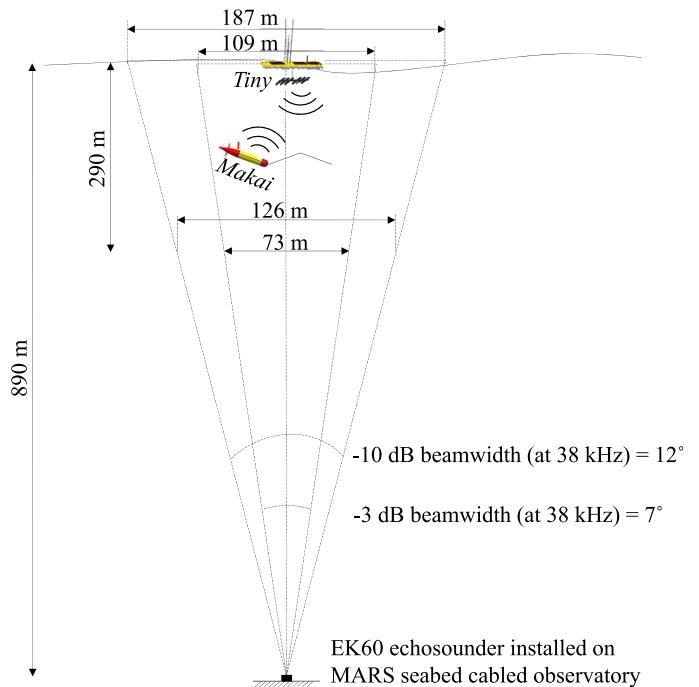


Fig. 2. Illustration of collaborative operation of LRAUV *Makai*, Wave Glider *Tiny*, and the seabed-mounted EK60 echosounder in the May–June 2019 experiment.

vertically migrating animals (see Section II). A station-keeping Wave Glider was deployed to mark the echosounder's latitude and longitude. To remain in the echosounder's beam, the LRAUV was required to acoustically track the Wave Glider at a horizontal distance within $\sim 100\text{ m}$, while the LRAUV took water samples from near surface down to $\sim 290\text{ m}$. Thus, the depth difference between the two vehicles was up to three times the horizontal distance, so it was no longer appropriate to use the slant range as the horizontal range. To meet this stringent tracking accuracy requirement, we improved the tracking algorithm as presented in Section III.

By closely tracking the Wave Glider that marked the echosounder's location, the LRAUV remained in the echosounder's beam while acquiring water samples at a sequence of depths. These samples were coregistered with the biological layers observed on the echogram. This was the first known effort of combining autonomous mobile eDNA sampling and simultaneous echosounder observation of biological features. The system performance is presented in Section IV. We conclude and outline future work in Section V.

II. EXPERIMENT SETUP

In a field experiment from May 29 to June 6, 2019, research vessels and autonomous platforms were deployed around the MARS site to collaboratively observe and sample the vertically migrating animals through both traditional and novel means. The LRAUV *Makai* equipped with a 3G-ESP was positioned within the echosounder's acoustic beam as shown in Fig. 2. *Makai* acquired water samples at a sequence of depths from near surface down to $\sim 290\text{ m}$ starting at 10 A.M. (or 10 P.M.) after the

dawn (or dusk) migration had completed. Before each sampling mission, scientists selected the sampling depths based on the real-time echogram from the seabed-mounted echosounder. The mission program with these depth settings was then transmitted to *Makai* via Iridium satellite when the vehicle was on the sea surface. Our objective was to adaptively sample the densest SSLs to identify their constituents via eDNA sequencing.

Our goal was to maintain *Makai* within the echosounder's "field of view" (i.e., within its main beam), so that the samples collected could be coregistered with the biological layers observed on the echogram. At the 38-kHz operating frequency, the echosounder's half power (i.e., -3 dB) beam width is 7° , corresponding to a beam cone of 109-m diameter at the sea surface and 73-m diameter at 290-m depth. The -10 -dB beam width is 12° , corresponding to a beam cone of 187-m diameter at the sea surface, and 126-m diameter at 290-m depth. Hence, *Makai* was required to navigate within a ~ 100 -m radius around the echosounder (based on the -10 -dB beam width). Beam angles were confirmed during a calibration using standard methods [25] in a 15-m-long, 10-m-wide, and 10-m-deep test tank at the Monterey Bay Aquarium Research Institute before deployment. As a navigation aid, a Liquid Robotics Wave Glider *Tiny* was deployed on the sea surface directly above the seabed-mounted echosounder, and circled around the echosounder location (36.71211°N , 122.18703°W) by closed-loop control based on GPS fixes. *Tiny*'s circle radius was set to 75 m, sufficiently large to prevent fast turns that could cause twists and excessive force on the umbilical cable between the surface float and the submerged "sub." *Makai* was equipped with a Teledyne Benthos DAT, and *Tiny* carried a Teledyne Benthos acoustic modem. In each sampling depth bin, *Makai* acoustically tracked *Tiny* while taking one water sample on a tight circular yo-yo trajectory (centered on *Tiny*'s location), as illustrated in Fig. 2.

III. LRAUV NAVIGATION AND SAMPLING ALGORITHMS

A. Estimating Acoustic Target's Latitude and Longitude From Range and Direction

During *Makai*'s sampling missions, *Makai* tracked *Tiny* as the acoustic target. *Makai*'s DAT was programmed to emit acoustic pulses every 25 s. When receiving *Makai*'s ping, *Tiny*'s modem sent a reply pulse back to *Makai*. *Makai*'s DAT received *Tiny*'s reply to estimate *Tiny*'s slant range and direction (azimuth and elevation angles), which were then transformed to *Tiny*'s coordinates in *Makai*'s vehicle reference frame. *Makai* used its own attitude and position to transform *Tiny*'s coordinates in *Makai*'s vehicle reference frame to latitude and longitude.

Noise in *Makai*'s DAT-measured elevation angle of *Tiny* would introduce errors when transforming *Tiny*'s slant range and direction to coordinates in *Makai*'s vehicle reference frame. In this experiment, *Tiny*'s depth was zero (on the sea surface) and *Makai*'s depth was known in real time. Hence, we devised a method of using the known depth difference of the two platforms rather than the elevation angle when transforming *Tiny*'s slant range and direction to its coordinates on *Makai*'s vehicle plane, as illustrated in Fig. 3. Suppose *Makai*'s pitch angle is θ and its roll angle is zero. *Tiny*'s location is projected onto the horizontal

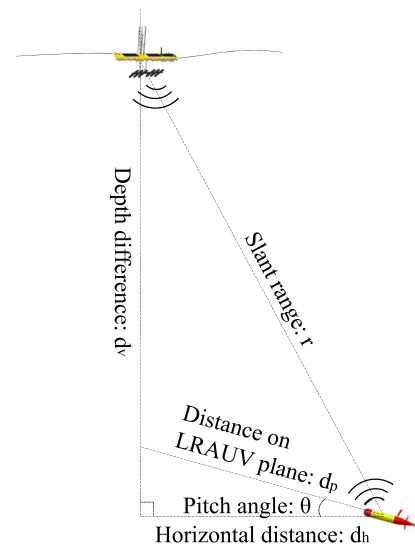


Fig. 3. Diagram of deriving the horizontal distance between LRAUV *Makai* and Wave Glider *Tiny* using the slant range and the depth difference (when *Tiny*'s azimuth angle from *Makai* is zero).

plane at a point with a horizontal distance d_h from *Makai*. The vertical projection line intersects the *Makai* vehicle plane at a point with a distance d_p from *Makai*. By the Pythagorean theorem, d_h is derived from the slant distance r and the two vehicles' depth difference (i.e., the vertical distance) d_v as follows:

$$d_h = \sqrt{r^2 - d_v^2}. \quad (1)$$

In general (see Fig. 11), when θ is small, d_p can be approximated by d_h , and the relative approximation error is

$$\frac{d_p - d_h}{d_p} \leq 1 - \cos(\theta).$$

The equal sign holds when *Tiny*'s azimuth angle from *Makai* is zero (which is the case shown in Fig. 3). In the experiment, on *Makai*'s yo-yo trajectory in the sampling missions, $\theta = \pm 20^\circ$. Thus, the maximum relative error of approximation was $1 - \cos(\pm 20^\circ) = 6\%$.

In one sampling mission from June 3 to 4, *Makai* acquired samples in a sequence of seven depth bins—35–40 m, 50–55 m, 100–105 m, 125–130 m, 150–155 m, 200–205 m, 250–255 m—as shown in Fig. 4. Each sample in each depth bin took about 1 h. *Tiny*'s slant range from *Makai* r as measured by *Makai*'s DAT is shown by the red dots in the upper panel. The horizontal distance d_h derived in real time using (1) is shown by the blue circles in the upper panel.

After *Tiny*'s coordinates were transformed from *Makai*'s vehicle reference frame to the Earth reference frame, the raw latitude and longitude estimates went through outlier rejection and low-pass filtering using a sliding window of five data points. In each set of five data points, the center latitude and longitude were calculated. The data point with the largest distance to the center was deemed an outlier and rejected, as shown in Fig. 5. The remaining four latitudes (and longitudes) were averaged to produce the low-pass filtered latitude (and longitude).

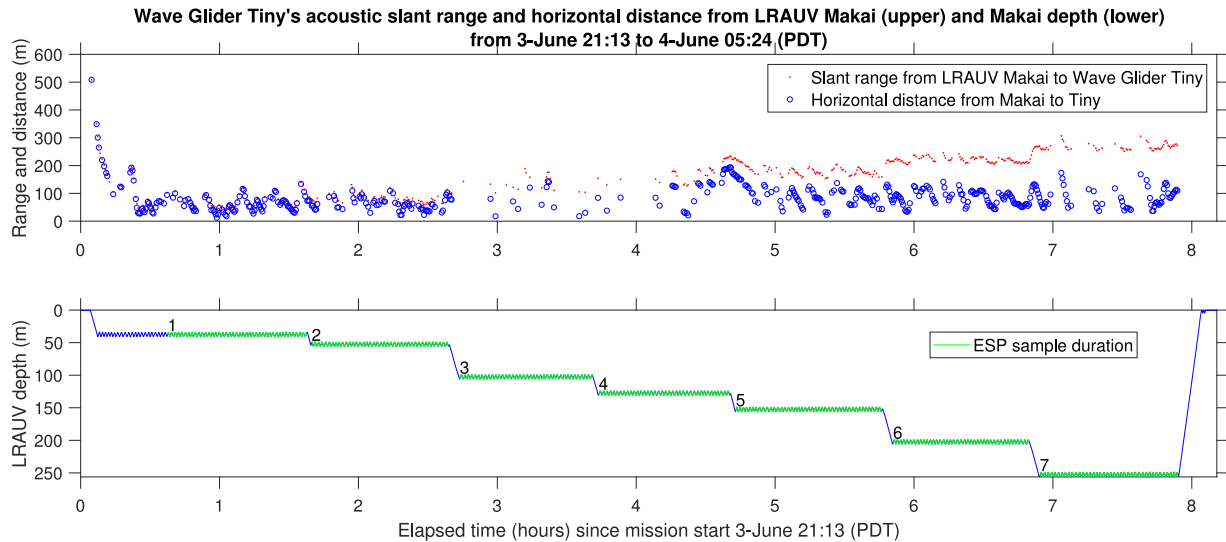


Fig. 4. Wave Glider *Tiny*'s slant range and horizontal distance from LRAUV *Makai* (upper) and *Makai*'s depth (lower) during a seven-sample mission. In the lower panel, the sample number marks the start of each sample's duration (green).

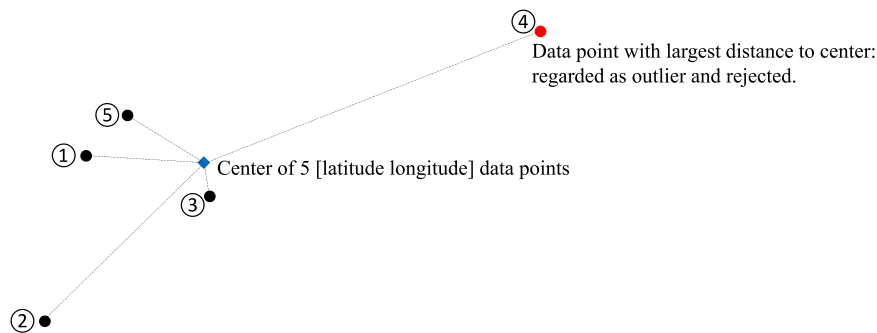


Fig. 5. Illustration of the algorithm of finding and rejecting the outlier in each set of five data points.

Tiny's latitude and longitude (raw and low-pass filtered) estimated by *Makai* during *Makai*'s sampling mission in the first depth bin (35–40 m) is shown in Fig. 6.

B. Tracking Acoustic Target While Sampling

In each 5-m sampling depth bin, *Makai* ran on a circular yo-yo trajectory (at 0.8-m/s speed and $\pm 20^\circ$ pitch angle) centered on *Tiny*'s estimated latitude and longitude at a programmed radius of 20 m. The lower panel of Fig. 6 shows *Makai*'s yo-yo trajectory in the first depth bin.

IV. SYSTEM PERFORMANCE

During a sampling mission, *Makai* estimated *Tiny*'s latitude and longitude based on the DAT-measured range and direction from *Makai* to *Tiny*, as well as *Makai*'s attitude and position. At the start of the mission, *Makai* logged its own GPS location before diving. Once underwater, *Makai* calculated its location based on the initial latitude and longitude and the estimated speed and the measured heading and attitude. In an ocean current, *Makai*'s dead-reckoned latitude and longitude deviated from the Earth-referenced counterparts because the vehicle

velocity used in the dead-reckoning calculation was relative to the water rather than the Earth. The same deviation was carried over to *Makai*-reckoned *Tiny* latitude and longitude because they were calculated based on *Makai*'s own dead-reckoned location. This deviation did not adversely affect *Makai*'s acoustic tracking of *Tiny* because the tracking was based on the relative locations of the two platforms, which carried the same deviation. However, to reconstruct *Makai*'s Earth-referenced trajectory for performance evaluation, we must remove the deviation.

Fig. 7 shows *Makai* and *Tiny*'s navigation performance in the first sampling depth bin. The upper and lower left panels show the latitudes and longitudes of *Makai* and *Tiny*, respectively. In this duration, there was a southward current. To counteract the current to stay below *Tiny*, *Makai* made a northward movement relative to the water, and hence its dead-reckoned latitude progressed northward while its Earth-referenced latitude did not. The current-induced deviation in latitude/longitude equals the difference between *Tiny*'s GPS latitude/longitude and *Tiny*'s latitude/longitude reckoned by *Makai*.

In the upper left panel of Fig. 7, *Tiny*'s GPS latitude and *Tiny*'s latitude reckoned by *Makai* are each low-pass filtered by a 11-min sliding window (the time for *Makai* to run four 20-m radius

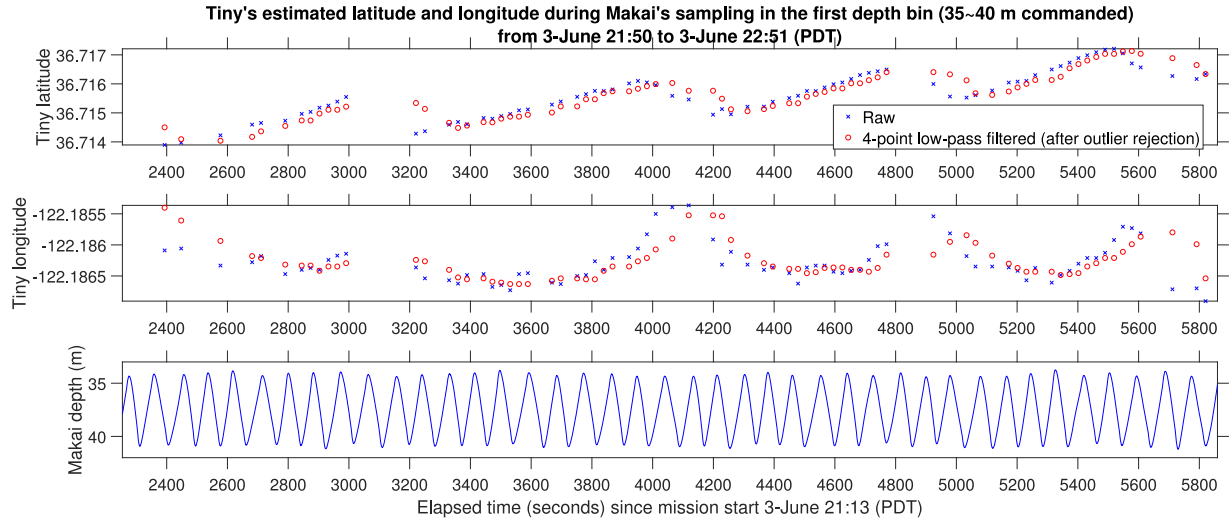


Fig. 6. *Tiny*'s estimated latitude and longitude (upper and middle panels) during *Makai*'s sampling mission in the first depth bin (*Makai*'s vertical trajectory shown in lower panel).

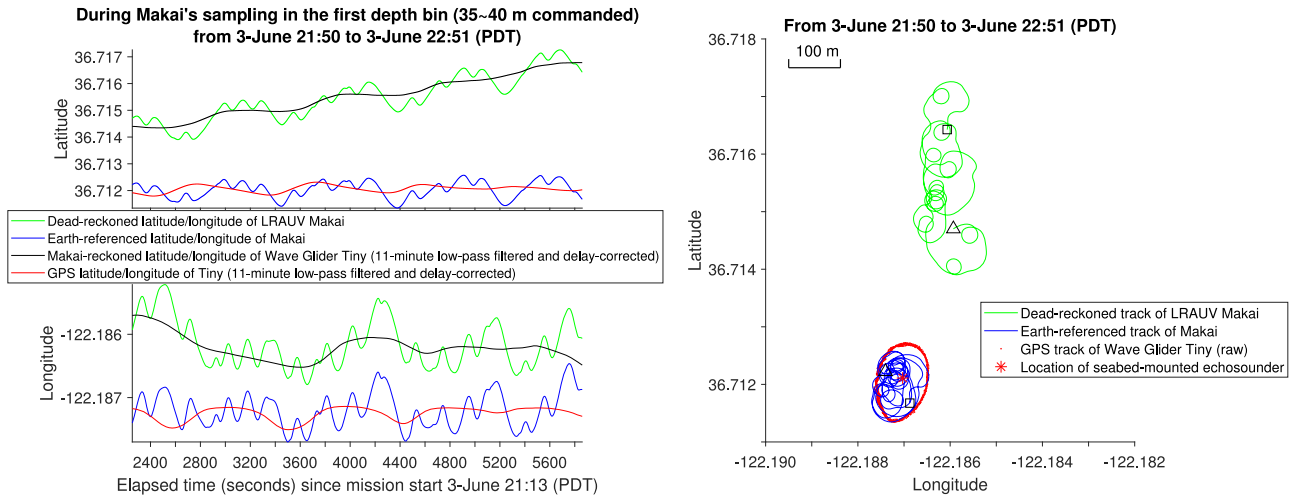


Fig. 7. *Makai* and *Tiny*'s latitudes and longitudes in *Makai*'s first sampling depth bin. In the right panel, *Makai*'s start and end locations are marked by the triangle and the square, respectively.

circles) to suppress short-term undulations. The difference of the two low-pass filtered quantities is taken as the current-induced latitude deviation. This deviation is removed from *Makai*'s dead-reckoned latitude to produce *Makai*'s Earth-referenced latitude. The longitudes are processed in the same way, as shown in the lower left panel. The plan view of *Makai*'s dead-reckoned and Earth-referenced tracks are shown in the right panel, along with *Tiny*'s GPS track. *Makai*'s Earth-referenced trajectory shows that it stayed near the echosounder location within a ~ 100 -m horizontal distance.

As shown in Fig. 4, the average horizontal distance between *Makai* and *Tiny* in the first sampling depth bin was about 60 m (the average over all seven samples was about 80 m), which was much larger than the desired 20 m in *Makai* mission setting. Considerations of this discrepancy are as follows. *Tiny* was circling around the echosounder location at an average speed of 0.48 m/s. *Makai*'s DAT acquired acoustic fixes of *Tiny* at an average interval of 1 min, which corresponded to about 30-m

traveled distance by *Tiny*. Once *Makai* received *Tiny*'s new location, *Makai* accordingly adjusted course to attempt to catch up with *Tiny* and circle around it. However, the 30-m lag led to an increased distance between the two vehicles. There were other error sources such as the DAT USBL ranging error.

A perspective view of *Makai*'s Earth-referenced trajectory over the entire seven-sample mission is shown in Fig. 8. Over the sampling duration in each depth bin, the average current velocity can be estimated based on *Makai*'s Earth-referenced and dead-reckoned latitudes and longitudes as follows:

$$V_{c_northward} = \frac{(\text{LatCorrection}_{\text{end}} - \text{LatCorrection}_{\text{start}}) \times R_{\text{Earth}}}{\text{duration}} \quad (2)$$

$$V_{c_eastward} = \frac{(\text{LonCorrection}_{\text{end}} - \text{LonCorrection}_{\text{start}}) \times R_{\text{Earth}} \times \cos(\text{Lat}_{\text{avg}})}{\text{duration}} \quad (3)$$

where

$$\text{LatCorrection} = \text{Earth-referenced latitude} - \text{dead-reckoned latitude}$$

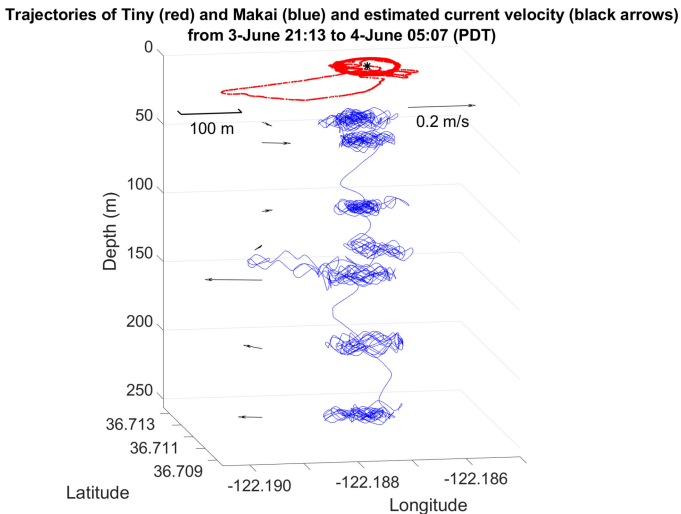


Fig. 8. *Makai* and *Tiny*'s trajectories during the seven-sample mission. The seabed-mounted echosounder's location (latitude and longitude) is marked by the asterisk.

$\text{LonCorrection} = \text{Earth-referenced longitude} - \text{dead-reckoned longitude}$.

The subscripts *start* and *end* refer to the start and the end of the duration, respectively. R_{Earth} is the radius of the Earth. Lat_{avg} is the average latitude in the duration. In the above calculations, latitude and longitude are in radians.

The estimated current velocities in the seven depth bins are shown in Fig. 8. Despite the significant velocities and the vertical shear of the current, *Makai* was able to stay near the echosounder location within a ~ 100 -m horizontal distance. It is noted that at the end of the fourth sample, *Tiny* briefly left the programmed circle, and *Makai* followed *Tiny*, so that they both deviated from the echosounder location. A likely cause was that *Tiny* got tangled by drifting kelp so that either the rudder was obstructed or the added drag from the kelp slowed the vehicle and caused it to drift with the ocean current. It appears that the kelp cleared itself and *Tiny* was able to return to the programmed circle after about 20 min.

Over 32 h from June 3 to 5, *Makai* completed three sampling missions (seven samples per mission). Fig. 9 shows the echogram recorded by the seabed-mounted echosounder during these missions. The color scale indicates the mean volume backscattering strength (S_v in dB re 1 m^{-1}). *Makai*'s yo-yo trajectory in each depth bin and the descent from one depth bin to the next is visible in the echogram as the bright narrow line of backscatter. All other backscatter was due to dispersed biological targets, likely including dispersed schools of small pelagic fish near the surface and a mixture of micronekton (identified in video surveys by a remotely operated vehicle as krill, siphonophores, lanternfish, sergestid shrimp, juvenile hake) in the deeper layers. In the duration of each depth bin, *Makai* acquired one water sample for eDNA analysis. The samples were coregistered with the biological layers recorded on the echogram.

The total 21 eDNA samples captured the biological layers formed after the dawn and dusk vertical migrations. The diel vertical migration of mesopelagic animals is clearly visible with

the descent of the main scattering layer at dawn and its ascent at dusk. A variety of other scattering structures are also visible, including at least eight thin layers, which formed shortly after the upward migration in the evening of June 4. Mission planning based on the real-time echogram allowed *Makai* to target several of these layers for sampling. The strong backscatter in the upper 20 m over 6 h on June 4 around 00:00 was due to small epipelagic fish, likely anchovy, feeding in dispersed shoals at night. Molecular analysis of the samples is currently underway.

In addition to collecting eDNA samples, *Makai* continuously measured temperature, salinity, chlorophyll, and dissolved oxygen as shown in Fig. 10. In between the three sampling missions, *Makai* ran on a circular yo-yo trajectory in the upper 50 m centered on *Tiny* to make measurements in the upper water column. These contextual data are important for understanding the environmental context of the animals' vertical migration. Since migrating animals may be targeting layers of prey, such as phytoplankton, knowing the physical structure of the water column can help us explain why we find certain animals at different depths. In Fig. 10, we see the thermocline was at about 50-m depth, and in the upper 30 m, there was a phytoplankton layer indicated by high chlorophyll.

V. CONCLUSION AND FUTURE WORK

In a field experiment in Monterey Bay during May–June 2019, a 3G-ESP LRAUV acquired eDNA samples at a sequence of depths from near surface down to ~ 290 m over diel cycles, directed by the distribution of animals observed in live data from a seabed-mounted echosounder. The LRAUV remained within the beam of the echosounder while collecting eDNA samples by acoustically tracking a station-keeping Wave Glider. This experiment demonstrated a new mode of persistent and simultaneous eDNA sampling and acoustic observation for studying the behaviors of vertically migrating animals. The molecular analysis of the samples (currently underway) will allow correlation of eDNA signals with the acoustic traces of the midwater animals over diel migration cycles.

After each sampling mission, the LRAUV ascended to the sea surface to receive the next set of sampling depths via satellite communications, and then dove to take samples accordingly from shallow to deepest bins. In some cases, the deeper scattering layers had shifted in position by the time the vehicle reached them. To mitigate that problem, we are currently developing acoustic messaging approaches so that sampling directives can be altered as needed without requiring the LRAUV to ascend to surface, using a sea-surface gateway (e.g., a Wave Glider or a buoy near the LRAUV) that relays shore commands via the satellite to the submerged vehicle via acoustics. By eliminating repeated surfacing and diving trips, the LRAUV's efficiency and accuracy of targeted sampling of biological features will be improved. In addition, we are developing an LRAUV algorithm that directly derives its Earth-referenced location when acoustically tracking a surface asset (e.g., a Wave Glider or a mooring), based on the LRAUV-measured range and direction of the surface asset as well as the surface asset's

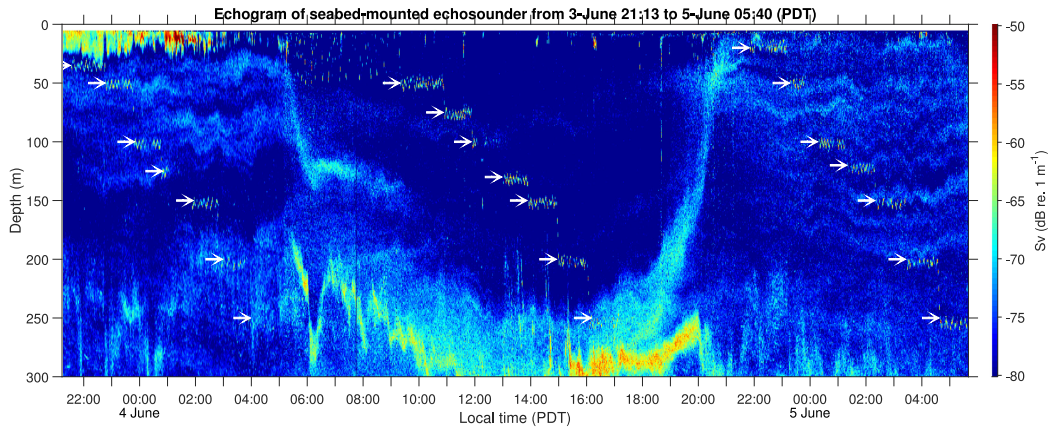


Fig. 9. Echogram from the seabed-mounted echosounder during *Makai's* three sampling missions (seven samples per mission). *Makai's* track in each sampling depth bin is marked by an arrow.

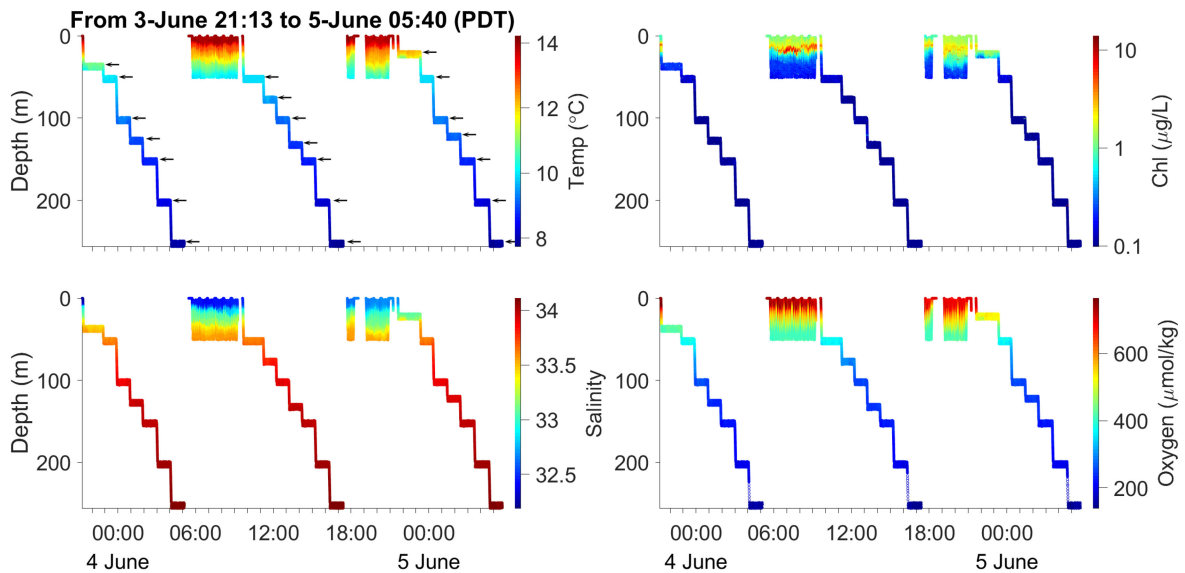


Fig. 10. *Makai*-measured temperature, salinity, chlorophyll, and dissolved oxygen during the three sampling missions. *Makai's* track in each sampling depth bin is marked by an arrow.

known GPS location transmitted to the LRAUV via acoustic messaging.

An echosounder was incorporated into a Wave Glider and an imaging Dorado AUV used in this study. Development of onboard decision making will realize real-time detection and classification of biological features, and inter-vehicle communications will enable transmitting this information to a 3G-ESP LRAUV for targeted sampling. The combination of these new capacities will free the acoustically directed sampling effort from a fixed geographic location, and expand the potential questions that can be addressed.

APPENDIX A

PROJECTIONS OF WAVE GLIDER LOCATION ONTO LRAUV PLANE AND HORIZONTAL PLANE

In Fig. 11, the LRAUV *Makai* and the Wave Glider *Tiny* are located at points M and T , respectively. The LRAUV plane

$AEMF$ is defined by *Makai's* forward direction MF and starboard direction ME . The angle between plane $AEMF$ and the horizontal plane $CEMG$ is *Makai's* pitch angle θ . *Makai's* roll angle is assumed to be zero. Fig. 11 illustrates the following orthogonal projections of point T onto the LRAUV plane and the horizontal plane.

- 1) The orthogonal projection of the Wave Glider location onto the LRAUV plane: point T is orthogonally projected onto plane $AEMF$ to point A . The distance between points M and T is the slant distance r measured by *Makai's* DAT. The angle between lines MF and MA is *Tiny's* azimuth angle α from *Makai*. The angle between lines MT and MA is *Tiny's* elevation angle γ from *Makai*.
- 2) The orthogonal projection of the Wave Glider location onto the horizontal plane: point T is orthogonally projected onto plane $CEMG$ to point D . The distance between points M and D is d_h . Line TD intersects the LRAUV plane $AEMF$ at point B .

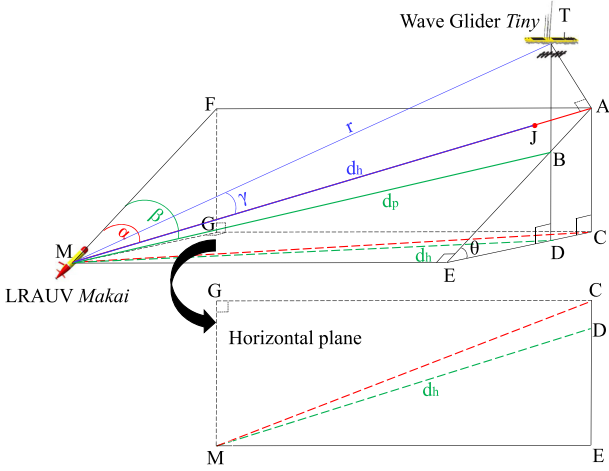


Fig. 11. Upper panel: perspective view of the projections of the Wave Glider *Tiny* location onto the LRAUV plane and the horizontal plane. Lower panel: plan view of the horizontal plane.

The distance between points M and B is d_p . The angle between lines MF and MB is denoted by β . Angles β and α generally differ (except for $\alpha = \beta = 0$ or π) but covary.

In the LRAUV algorithm for estimating *Tiny*'s location, the DAT-measured azimuth angle α was used but the elevation angle γ was ignored (i.e., the elevation angle was deemed zero); the distance d_h was calculated using the known depth difference of the two platforms [see (1)]. Therefore, *Makai* reckoned that *Tiny* was at point J on line MA , at a distance d_h from point M . However, point B was *Tiny*'s actual intersecting point on plane $AEMF$ (on projection line TD), on line MB at a distance d_p from point M . Point B 's coordinates in *Makai*'s vehicle reference frame would be transformed to *Tiny*'s actual latitude and longitude. Using point J instead of point B in this transformation generally introduces an error in *Tiny*'s latitude and longitude estimates. The distance error $d_p - d_h$ and the angle error $\beta - \alpha$ are derived as follows.

A. Distance Error

In the right triangle BDM , the relation between d_p and d_h is

$$d_p^2 = d_h^2 + BD^2 \quad (4)$$

In the right triangle BDE

$$BD = BE \sin(\theta). \quad (5)$$

In the right triangle BEM

$$BE = d_p \cos(\beta). \quad (6)$$

Incorporating (6) into (5), and then into (4), we have

$$d_p^2 = d_h^2 + d_p^2 \sin^2(\theta) \cos^2(\beta). \quad (7)$$

Solving for d_p , we have

$$d_p = d_h \sqrt{\frac{1}{1 - \sin^2(\theta) \cos^2(\beta)}}. \quad (8)$$

Noting that

$$\begin{aligned} 1 - \sin^2(\theta) \cos^2(\beta) &= \sin^2(\beta) + \cos^2(\beta) - \sin^2(\theta) \cos^2(\beta) \\ &= \sin^2(\beta) + \cos^2(\beta) \cos^2(\theta) \end{aligned}$$

(8) is rewritten as

$$d_p = d_h \sqrt{\frac{1}{\sin^2(\beta) + \cos^2(\beta) \cos^2(\theta)}}. \quad (9)$$

Noting that

$$\begin{aligned} \frac{1}{\sin^2(\beta) + \cos^2(\beta) \cos^2(\theta)} &= \frac{\sin^2(\beta) + \cos^2(\beta)}{\sin^2(\beta) + \cos^2(\beta) \cos^2(\theta)} \\ &= \frac{1 + \tan^2(\beta)}{\cos^2(\theta) + \tan^2(\beta)} \end{aligned}$$

we have

$$d_p = d_h \sqrt{\frac{1 + \tan^2(\beta)}{\cos^2(\theta) + \tan^2(\beta)}}. \quad (10)$$

When approximating d_p by d_h , the relative error is

$$\frac{d_p - d_h}{d_p} = 1 - \sqrt{\frac{\cos^2(\theta) + \tan^2(\beta)}{1 + \tan^2(\beta)}}. \quad (11)$$

The above error reaches the maximum value $1 - \cos(\theta)$ when $\beta = 0$ or π (i.e., when $\alpha = 0$ or π).

B. Angle Error

Considering the right triangles AMT and AEM , we have

$$AE = r \cos(\gamma) \cos(\alpha) \quad (12)$$

$$ME = r \cos(\gamma) \sin(\alpha). \quad (13)$$

Considering the right triangles AMT and ABT , we have

$$AB = r \sin(\gamma) \tan(\theta). \quad (14)$$

In the right triangle BEM

$$\beta = \arctan\left(\frac{ME}{AE - AB}\right) \quad (15)$$

$$= \arctan\left[\frac{\sin(\alpha)}{\cos(\alpha) - \tan(\gamma) \tan(\theta)}\right] \quad (16)$$

where (12)–(14) are used.

The angle error is

$$\beta - \alpha = \arctan\left[\frac{\sin(\alpha)}{\cos(\alpha) - \tan(\gamma) \tan(\theta)}\right] - \alpha. \quad (17)$$

When $\theta = 0$ or $\gamma = 0$, the angle error is zero. The angle error increases with θ and γ .

ACKNOWLEDGMENT

The authors would like to thank J. G. Bellingham for initiating the LRAUV program; M. Godin, J. Erickson, R. McEwen, M. Chaffey, E. Mellinger, D. Klimov, T. Hoover, T. O'Reilly, and E. Trauschke for contributions to the LRAUV development; M. J. Stanway for contributions to the earlier work of installing

a DAT on an LRAUV and using it to track and home to an acoustic target; J. Ryan for improving the real-time LRAUV data decimation and displaying algorithm; D. Pargett, S. Jensen, W. Ussler, K. Yamahara, and R. Marin III for contributions to the 3G-ESP development. They would also like to thank Kongsberg Simrad and J. Horne (University of Washington) for loaning the EK60 echosounder; C. Waluk for assistance with its refurbishment and deployment; C. Wahl for helping with the Wave Glider operation and providing its GPS data; C. Rueda, J. Winnikoff, R. Michisaki, K. Yamahara, R. Marin III, W. Ussler, S. Johnson, K. Walz, B. Jones, and S. Haddock for helping with the LRAUV operation; and K. Gomes for managing the MBARI ODSS (Oceanographic Decision Support System) during the experiment.

REFERENCES

- [1] R. S. Dietz, "The sea's deep scattering layers," *Sci. Amer.*, vol. 207, no. 2, pp. 44–51, 1962.
- [2] G. C. Hays, "A review of the adaptive significance and ecosystem consequences of zooplankton diel vertical migrations," *Hydrobiologia*, vol. 503, pp. 163–170, 2003.
- [3] R. S. Dietz, "Deep scattering layer in the Pacific and Antarctic Oceans," *J. Mar. Res.*, vol. 7, no. 3, pp. 430–442, 1948.
- [4] E. G. Barham, "The ecology of sonic scattering layers in the Monterey Bay area," Ph.D. dissertation, Hopkins Mar. Station, Stanford Univ., Pacific Grove, CA, USA, Feb. 1957.
- [5] C. Robinson *et al.*, "Mesopelagic zone ecology and biogeochemistry—A synthesis," *Deep Sea Res. II*, vol. 57, pp. 1504–1518, 2010.
- [6] O. Aumont, O. Maury, S. Lefort, and L. Bopp, "Evaluating the potential impacts of the diurnal vertical migration by marine organisms on marine biogeochemistry," *Global Biogeochem. Cycles*, vol. 32, no. 11, pp. 1622–1643, 2018.
- [7] J. K. Horne, "Acoustic approaches to remote species identification: A review," *Fisheries Oceanogr.*, vol. 9, no. 4, pp. 356–371, 2000.
- [8] J. Simmonds and D. MacLennan, *Fisheries Acoustics: Theory and Practice*, 2nd ed. Oxford, U.K.: Blackwell Sci., 2005.
- [9] P. F. Thomsen, J. Kielgast, L. L. Iversen, P. R. Møller, M. Rasmussen, and E. Willerslev, "Detection of a diverse marine fish fauna using environmental DNA from seawater samples," *PLoS One*, vol. 7, no. 8, 2012, Art. no. e41732.
- [10] J. K. Horne, S. S. Urmy, and D. H. Barbee, "Using sonar to describe temporal patterns of oceanic organisms from the MARS observatory," in *Proc. MTS/IEEE OCEANS Conf.*, Sep. 2010, pp. 1–7.
- [11] K. J. Benoit-Bird and G. L. Lawson, "Ecological insights from pelagic habitats acquired using active acoustic techniques," *Annu. Rev. Mar. Sci.*, vol. 8, pp. 463–490, 2016.
- [12] K. G. Foote, "Linearity of fisheries acoustics, with addition theorems," *J. Acoust. Soc. Amer.*, vol. 73, no. 6, pp. 1932–1940, Jun. 1983.
- [13] D. M. Pargett, J. M. Birch, C. M. Preston, J. P. Ryan, Y. Zhang, and C. A. Scholin, "Development of a mobile ecogenomic sensor," in *Proc. MTS/IEEE OCEANS Conf.*, Oct. 2015, pp. 1–6.
- [14] C. Scholin *et al.*, "The quest to develop ecogenomic sensors: A 25-year history of the Environmental Sample Processor (ESP) as a case study," *Oceanography*, vol. 30, no. 4, pp. 100–113, 2017.
- [15] K. M. Yamahara *et al.*, "In situ autonomous acquisition and preservation of marine environmental DNA using an autonomous underwater vehicle," *Frontiers Mar. Sci.*, vol. 6, 2019, pp. Art. no. 373.
- [16] B. Hobson, J. G. Bellingham, B. Kieft, R. McEwen, M. Godin, and Y. Zhang, "Tethys-class long range AUVs - extending the endurance of propeller-driven cruising AUVs from days to weeks," in *Proc. IEEE AUV*, Sep. 2012, pp. 1–8.
- [17] J. G. Bellingham *et al.*, "Efficient propulsion for the Tethys long-range autonomous underwater vehicle," in *Proc. IEEE AUV*, Sep. 2010, pp. 1–6.
- [18] J. G. Bellingham and T. R. Consi, "State configured layered control," in *Proc. IARP 1st Workshop Mobile Robots Subsea Environ.*, Oct. 1990, pp. 75–80.
- [19] M. A. Godin, J. G. Bellingham, B. Kieft, and R. McEwen, "Scripting language for state configured layered control of the Tethys long range autonomous underwater vehicle," in *Proc. MTS/IEEE OCEANS Conf.*, Sep. 2010, pp. 1–7.
- [20] H. Singh *et al.*, "An integrated approach to multiple AUV communications, navigation, and docking," in *Proc. MTS/IEEE OCEANS Conf.*, Sep. 1996, pp. 59–64.
- [21] M. J. Stanway, B. Kieft, T. Hoover, B. Hobson, A. Hamilton, and J. Bellingham, "Acoustic tracking and homing with a long-range AUV," in *Proc. MTS/IEEE OCEANS Conf.*, Sep. 2014, pp. 1–7.
- [22] Y. Zhang *et al.*, "Isotherm tracking by an autonomous underwater vehicle in drift mode," *IEEE J. Ocean. Eng.*, vol. 42, no. 4, pp. 808–817, Oct. 2017.
- [23] T. C. O'Reilly, B. Kieft, and M. Chaffey, "Communications relay and autonomous tracking applications for Wave Glider," in *Proc. IEEE OCEANS Conf.*, May 2015, pp. 1–6.
- [24] Y. Zhang *et al.*, "Autonomous tracking and sampling of the deep chlorophyll maximum layer in an open-ocean eddy by a long-range autonomous underwater vehicle," *IEEE J. Ocean. Eng.*, early access, doi:10.1109/OJOE.2019.2920217.
- [25] K. G. Foote, H. P. Knudsen, G. Vestnes, D. N. MacLennan, and E. J. Simmonds, "Calibration of acoustic instruments for fish density estimation: A practical guide," Int. Council Exploration Sea, Copenhagen, Denmark, Tech. Rep. Cooperative Res. Rep. no. 144, 1987.



Yanwu Zhang (Senior Member, IEEE) was born in 1969 in Shaanxi Province, China. He received the B.S. degree in electrical engineering and the M.S. degree in underwater acoustics engineering from Northwestern Polytechnic University, Xi'an, China, in 1989 and 1991, respectively, the M.S. degree in electrical engineering and computer science from the Massachusetts Institute of Technology (MIT), Cambridge, MA, USA, in 1998, and the Ph.D. degree in oceanographic engineering from the MIT/Woods Hole Oceanographic Institution (WHOI) Joint Program, Woods Hole, MA, USA, in 2000.

From 2000 to 2004, he was a Systems Engineer working on medical image processing with the General Electric Company Research and Development Center, Niskayuna, NY, USA, and then a Senior Digital Signal Processing Engineer working on digital communications at Aware Inc., Bedford, MA, USA. Since December 2004, he has been with the Monterey Bay Aquarium Research Institute, Moss Landing, CA, USA, first as a Senior Research Specialist and then as a Senior Research Engineer. He leads the project of targeted sampling by autonomous vehicles, designs adaptive sampling algorithms for marine ecosystem studies, and participated in the development of the Tethys-class long-range autonomous underwater vehicles (AUVs). Since 1996, he has participated in more than a dozen field experiments running the Odyssey IIB, Dorado, and Tethys AUVs.

Dr. Zhang is a member of Sigma Xi. He was a finalist of the *MIT Technology Review Magazine's* 100 young innovators (TR100) in 1999 when he was a Ph.D. student. In 2018, he was awarded the Visiting Fellowship of Antarctic Gateway Partnership from the University of Tasmania, Australia.

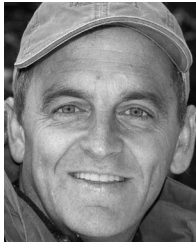


Brian Kieft received the B.S. degree in computer science from the Hope College, Holland, MI, USA, in 2001.

He worked in the avionics industry, developing and testing subsystems for military aircraft from 2001 to 2006. In 2006, he joined the Monterey Bay Aquarium Research Institute (MBARI), Moss Landing, CA, USA, as a Software Engineer. He has worked on various platforms, including mooring controllers, benthic instruments, Wave Gliders, and several AUVs and their associated payloads. He is currently working on

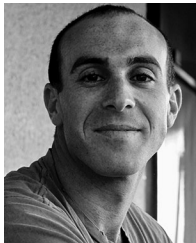
the development of the Tethys-class AUV—a long-range, upper-water-column AUV designed primarily for biological sensing. Apart from development, he also takes part in mission planning and payload integration for ongoing collaborative field programs and engineering tests. He has also been actively involved in updating and teaching the IEEE tutorial "AUV Technology and Application Basics" since 2011.

Mr. Brian is the Co-Chair of the Wave Glider users group.



Brett W. Hobson received the B.S. degree in mechanical engineering from San Francisco State University, San Francisco, CA, USA, in 1989.

He began his ocean engineering career with Deep Ocean Engineering, San Leandro, CA, USA, developing remotely operated vehicles. In 1992, he helped start and run Deep Sea Discoveries where he helped develop and operate deep-towed sonar and camera systems offshore the United States, Venezuela, Spain, and the Philippines. In 1998, he joined Nekton Research in North Carolina to design and deploy bio-inspired underwater vehicles for navy applications. After the sale of Nekton Research to iRobot in 2005, he joined the Monterey Bay Aquarium Research Institute (MBARI) where he leads the Long Range Autonomous Underwater Vehicle (AUV) program overseeing the development and science operations of six mega-meter range AUVs. His team has also developed MBARI's long-endurance seafloor crawling Benthic Rover. He teaches AUV tutorials for IEEE/MTS Oceans conferences each year, holds one patent, and is currently a Co-PI on NASA and NSF projects aimed at developing novel underwater vehicles for ocean science.



Ben-Yair Raanan received the B.S. degree in marine science from the Ruppin Academic Center, Israel, in 2011, and the M.S. degree in marine science from the Physical Oceanography Lab, Moss Landing Marine Laboratories, San Jose State University, San Jose, CA, USA, in 2014.

He is currently a Software Engineer with the Monterey Bay Aquarium Research Institute (MBARI), Moss Landing, CA, USA. He joined MBARI in 2014 as a Core Developer for MBARI's fleet of autonomous underwater vehicles, and works closely with researchers from a variety of disciplines to develop new enabling technologies for oceanographic research and exploration. His research interests include software design for autonomous robotic systems, machine learning, and artificial intelligence.



Samuel S. Urmy received the Bachelor of Science degree in Earth systems from Stanford University, Stanford, CA, USA, in 2008, the Master of Science degree in aquatic and fishery sciences from the University of Washington, Seattle, WA, USA, in 2012, and the Ph.D. degree in marine and atmospheric sciences from the State University of New York at Stony Brook, Stony Brook, NY, USA, in 2017.

After completing a postdoctoral fellowship at the Monterey Bay Aquarium Research Institute, he is currently a Research Fisheries Biologist, NOAA's Alaska Fisheries Science Center, Seattle, WA, USA. He is a Marine Ecologist and Biological Oceanographer and his research interests include how marine animals move through and inhabit their patchy unpredictable environment. To get answers to these questions, he uses active remote sensing (radar and sonar), modeling, and ecological theory. He has conducted field work in a variety of systems, from zooplankton in alpine lakes, to seabirds at the ocean's surface, to lanternfish in the mesopelagic zone.



Kathleen J. Pitz received the B.A. degree in molecular cell biology, emphasis in genetics, genomics, and developmental biology, from the University of California, Berkeley, Berkeley, CA, USA, in 2009, and the Ph.D. degree in biological oceanography from the Joint Program in Oceanography and Applied Ocean Science and Engineering, Woods Hole Oceanographic Institution and Massachusetts Institute of Technology, Woods Hole, MA, USA, in 2016.

She completed three years of a postdoctoral fellowship at the Monterey Bay Aquarium Research Institute, Moss Landing, CA, USA, where she is currently a Research Associate. Her research includes examining how environmental DNA (eDNA) relates to traditional measures of biodiversity, using eDNA to examine patterns of biodiversity and community change through time in Monterey Bay (on interannual to daily scales of variation) as well as how eDNA can be used to survey biodiversity regionally across the California Current Ecosystem.



Christina M. Preston received the B.S. degree in biology from James Madison University, Harrisonburg, VA, USA, in 1992 and the Ph.D. degree in ecology, evolution, and marine biology from the University of California, Santa Barbara, CA, USA, in 1998.

After the Ph.D., she was a postdoctoral scholar with Stanford University's Hopkins Marine Station, Pacific Grove, CA, USA. She is currently a Research Specialist with the Monterey Bay Aquarium Research Institute, Moss Landing, CA, USA. Her current research activities involve developing molecular methods to identify and quantify plankton *in situ* using underwater robots.



Brent Roman was born in Canton, IL, USA, in 1963. He received the B.S. degree in computer and information sciences from the University of California at Santa Cruz, Santa Cruz, CA, USA, in 1985.

His career as a Software Engineer began when he was a teenager working on automated concrete ready-mix batching systems coded in 8085 assembly language. He paid for the university by coding video tape editor controllers in Z-80 assembly. After the B.S. degree, he did a six-year stint marketing CAE software course. In 1990, he returned to product development, working on a small team creating a prototyping tool to aid in the design of automotive and aerospace digital servo control systems. In 1997, he joined the Santa Cruz Operation, where he specialized in the use of Unix and Linux on small PCs and embedded systems. He joined the Monterey Bay Aquarium Research Institute (MBARI) in 2000, where he focused on distributed control systems, communications, and software development for the Environmental Sample Processor.



Kelly J. Benoit-Bird received the B.S. degree in aquatic ecology from Brown University, Providence, RI, USA, in 1998, and the Ph.D. degree in zoology from the University of Hawaii at Manoa, Honolulu, HI, USA, in 2003.

She spent a year as a Postdoctoral Fellow at the Hawaii Institute of Marine Biology before joining the faculty of Oregon State University, in 2004, where she was a Professor of Oceanography until 2016. She is currently a Senior Scientist with the Monterey Bay Aquarium Research Institute, Moss Landing, CA, USA. Her research uses sound to explore the ecological role of spatial and temporal dynamics in pelagic marine ecosystems from the surface to the deep sea.

Dr. Benoit-Bird is a Fellow of the Acoustical Society of America, an Associate Editor for Limnology and Oceanography, and an IEEE Oceanic Engineering Society Distinguished Lecturer. She has recently served on the Scientific Steering Committee for the International Council for the Exploration of the Sea Symposium on Marine Ecosystem Acoustics, as an organizer for the National Academy of Sciences Kavli Frontiers of Science Symposium, and was the Chief Scientist for the Office of Naval Research Basic Research Challenge.



James M. Birch received the B.S. degree in zoology from The University of North Carolina, Chapel Hill, Chapel Hill, NC, USA, in 1983, and the M.S. and Ph.D. degrees in biology from the University of Michigan, Ann Arbor, MI, USA, in 1995.

He is currently the Director of the SURF Center, Monterey Bay Aquarium Research Institute, Moss Landing, CA, USA. The SURF Center (Sensors; Underwater Research of the Future) is a program that shepherds the development, deployment, and advancement of the Environmental Sample Processor (ESP), a robotic, autonomous microbiology laboratory that automates sample acquisition, processing, and analysis. Versions of the ESP have been deployed around the world's oceans, and recently have been used as a sampling instrument in our nation's freshwater streams collecting data on invasive species and helping with fish stock assessments. His research interests include technology development for the ocean sciences with crossover capabilities to freshwater/terrestrial realms.



Francisco P. Chavez was born and raised in Peru. He received the B.S. degree from Humboldt State University, Arcata, CA, USA and the Ph.D. degree from Duke University, Durham, NC, USA.

He is currently a Biological Oceanographer interested in how climate variability and change regulate ocean ecosystems on local and basin scales. He is a founding member of the Monterey Bay Aquarium Research Institute, Moss Landing, CA, USA, where he has pioneered time-series research and the development of new instruments and systems to make this type of research sustainable. He has authored more than 200 peer-reviewed papers with ten in *Nature* and *Science*.

Dr. Chavez is a Fellow of the American Association for the Advancement of the Sciences; honored for distinguished research on the impact of climate variability on oceanic ecosystems and global carbon cycling. He is also a Fellow of the American Geophysical Union; honored for advancing fundamental knowledge of the physical-biological coupling between Pacific Decadal Oscillations, productivity, and fisheries. He is a past member of the U.S. National Science Foundation Geosciences Advisory Committee, has been involved in the development of the U.S. Integrated Ocean Observing System, and is a member of the Governing Board of the Central and Northern California Coastal Ocean Observing System and the Science Advisory Team for the California Ocean Protection Council. He was awarded the *Doctor Honoris Causa* by the Universidad Nacional Pedro Ruiz Gallo, Lambayeque, Peru, in recognition of his distinguished scientific career and for contributing to elevate academic and cultural levels of university communities in particular and society in general. He was the 2014 recipient of the Ed Ricketts Memorial award.



Christopher A. Scholin received the bachelor's degree in biology from the University of California, Santa Barbara, Santa Barbara, CA, USA, the master's degree in molecular biology and immunology from Duke University, Durham, NC, USA, and the Ph.D. degree in biological oceanography from the Massachusetts Institute of Technology/Woods Hole Oceanographic Institution Joint Program, Woods Hole, MA, USA, in 1992.

His research at Monterey Bay Aquarium Research Institute, Moss Landing, CA, USA, focuses on the development of ecogenomic sensors for detecting water-borne micro-organisms and environmental DNA using molecular probe technology.

Dr. Scholin serves on the Board of Trustees of the Monterey Bay Aquarium Foundation and the Consortium for Ocean Leadership.